

# STIS/CCD Time Series Photometry with Saturated Data

---

Ronald L. Gilliland  
July 30, 1999

---

## ABSTRACT

*STIS/CCD data were acquired in a time series mode on  $\alpha$  Cen A & B to test limitations to ultra high Signal to Noise (S/N) capabilities. In order to reach a Poisson limited noise level of nearly 40,000 on  $\alpha$  Cen A the data were acquired in a spectral mode to spread the image over a full row of pixels, and with an exposure time that led to strong over-saturation. Each 10s exposure resulted in detection of  $\sim 1.5 \times 10^9 e^-$  for  $\alpha$  Cen A and  $\sim 2 \times 10^8 e^-$  for  $\alpha$  Cen B, with the latter spectrum just at saturation in some spectral regions. I discuss the data characteristics in detail and present time series results under a reasonable analysis approach. Simple interpretations from this one orbit of calibration data are hindered as a result of unusually large instrument drifts. A S/N greater than 9400 per exposure was reached for  $\alpha$  Cen A, and greater than 6800 for  $\alpha$  Cen B.*

---

## 1. Introduction

In principle CCD observations made from above the Earth's atmosphere, and hence free of atmospheric scintillation and transparency variations can provide ultrahigh S/N photometry. With a stable instrument time series results may reach S/N levels close to Poisson statistics limits, even at S/N well in excess of 10,000 corresponding to the collection of over  $10^8$  photo-electrons per exposure. CAL/STIS-8438 was designed as a one orbit test of S/N limitations for CCD time-series photometry. By observing simultaneously two stars differing by a factor of about seven in brightness (at the 3305 Å wavelength setting used), it was possible to expose the fainter  $\alpha$ Cen B to a level near saturation and have  $\alpha$  Cen A exposed well past saturation. The previous results of CAL/STIS-7666 (Gilliland, Goudfrooij, and Kimble 1999) had established that the CCD response remained linear to large over-saturation levels simply by summing over the electrons that bled into adjacent

columns. This linear response motivated a test of ultrahigh time series stability using the larger count levels provided by saturated data.

Although by normal standards a S/N of 10000 per exposure is very high, the science of asteroseismology would benefit from yet higher values. The Sun is observed to oscillate in a large number of closely spaced modes with periods near 5 minutes and amplitudes (in the optical) up to  $\sim 4$  ppm (parts per million). A marginal  $4\text{-}\sigma$  detection of such modes would therefore require power spectra with noise levels of 1 ppm. At a S/N per exposure of 10000 it would take 10000 exposures to provide a one-sigma noise level of 1 ppm. Since the gain with number of exposures goes only as  $\sqrt{N}$ , where  $N$  is the number of exposures, a gain in the S/N per exposure provides a gain as  $N^2$  in the number of exposures required to reach a given noise level. For the case of reaching 1 ppm, and assuming actual STIS/CCD overhead times it would take about 70 (CVZ) orbits at  $S/N = 10000$ , but only 18 orbits if the S/N per exposure could be raised to 20000. At the S/N of 3250 demonstrated from CAL-STIS-7666 it would require an unrealistic 660 orbits to reach a limiting noise level of 1 ppm (the level of  $S/N \sim 3250$  happens to be near the best demonstrated using large ground-based telescopes -- Gilliland *et al.* 1993). With 10-m class telescopes at a good ground-based site (e.g. Keck) a S/N of  $\sim 5000\text{-}6000$  should be possible for 10s exposures averaged over 8 hour observing windows. There are of course many stars that should have oscillations at amplitudes above that of the Sun, but for robust study of stellar interiors that can follow from detection of several oscillation modes the level of 1 ppm noise is a requirement for near solar analogues.

## 2. Observations

CAL/STIS-8438 executed 1999 May 15 in one standard (i.e., not CVZ) orbit. The observations have root names: o5i3010[2-9]. The total time spanned by the time series is 36 minutes. A total of 64 nominally identical 10 second exposures were obtained as a series of 8 sets of CR-SPLIT=8 logsheet lines.  $\alpha$  Cen A & B were selected for observations for several reasons:

1. Although no science could result from this one orbit test, it made sense to test with observations of a high priority science target.  $\alpha$  Cen A given its proximity, binary membership and close to solar properties has been a target for several (none yet successful) ground-based observing runs.
2. A pair of stars is desired to provide further diagnostics on any excess noise seen, e.g., correlated noise in both stars could indicate shutter timing variations, or perhaps drifts in the CCD gain.
3. The stars should be bright enough to provide count levels near saturation for the fainter star, and several times saturation for the brighter in an exposure time of about 10 s (long enough that 0.0002 s shutter timing fluctuations are not important, still short compared to the 20 s per exposure overhead time). This should be true using a medium resolution grating which can provide a flat spectral response over

the full wavelength range (3162 - 3448 Å in this case). Ideally this should hold for a near UV wavelength where the intrinsic amplitude of oscillations is expected to be somewhat larger. The combination of near- and over-saturated spectra is also useful for allowing quantification of how associated parameters that may correlate with added noise (like cross-dispersion position and width) vary in time, these can be developed from the unsaturated spectrum, but not from the saturated case with useful accuracy.

4. Previous observations of the stars should have established that intrinsic variations do not exist to levels below the per exposure precision limit (25 ppm in this case).

With use of G430M at the central wavelength of 3305Å these constraints are all well satisfied using  $\alpha$  Cen A & B. A 10 s exposure reaches close to saturation on  $\alpha$  Cen B, and provides times 7 over-saturation on  $\alpha$  Cen A. The orbital separation of  $\alpha$  Cen A & B is about 14".5 . By selecting a telescope orient which places A & B just slightly offset from each other in cross-dispersion it is possible to observe both in slit-less mode simultaneously while using a small (128 in this case) cross-dispersion subarray to minimize overheads. With a declination of -60 degrees  $\alpha$  Cen also passes through the CVZ for HST allowing for the possibility of very efficient observations. (The addition of an orient restriction to place A & B nearly along the STIS/CCD dispersion direction leads to CVZ passages only in May of even numbered years.)

Figure 1 shows one of the 1024x128 spectral images. The spectrum of  $\alpha$  Cen A is about 30 pixels above the  $\alpha$  Cen B spectrum. Depending upon position in the spectrum the  $\alpha$  Cen A spectrum saturates typically 5 to 20 pixels in cross-dispersion, while the  $\alpha$  Cen B spectrum only saturates the central pixel over limited regions of the spectrum.

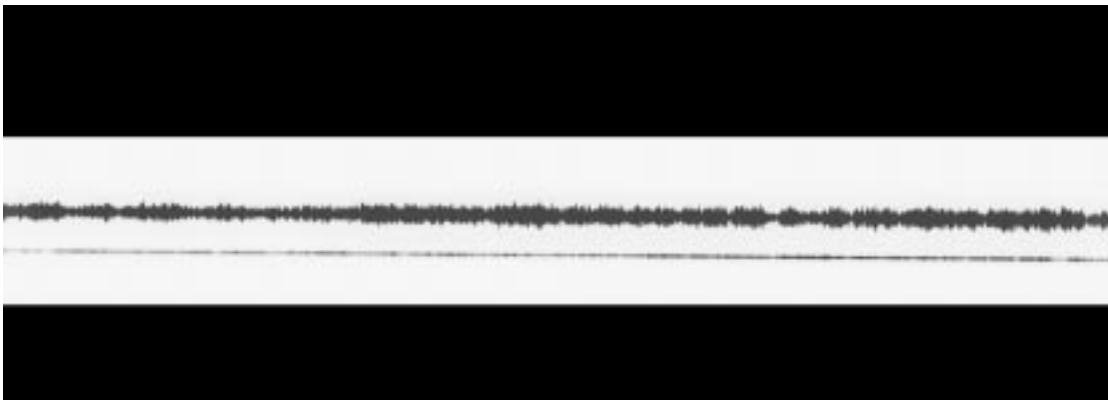


**Figure 1:** Direct image of 10 second spectroscopic exposure showing spectrum of  $\alpha$  Cen A on top and  $\alpha$  Cen B toward bottom of the 128 pixel STIS/CCD subarray.

### 3. Data Characteristics

The 64 spectra were all obtained using the gain of  $4 e^- DN^{-1}$  which provides excellent linearity beyond saturation. No dithering of position was commanded.

The raw data have overscan columns 18 deep on each end of the spectrum. I have derived means of the overscan regions, subtracted this from the 2-d data arrays and multiplied by 4 to create overscan subtracted frames in  $e^-$  units. As a check of the background level, means in the data area near the top of the subarray were developed for all 64 exposures. The *rms* of the data area background means was  $0.7 e^-$  per pixel, compared to a measurement precision of  $\sim 0.13 e^-$  per pixel. This fluctuation summed over extraction boxes for either  $\alpha$  Cen A or  $\alpha$  Cen B is near expected fluctuations from Poisson statistics on the objects alone.

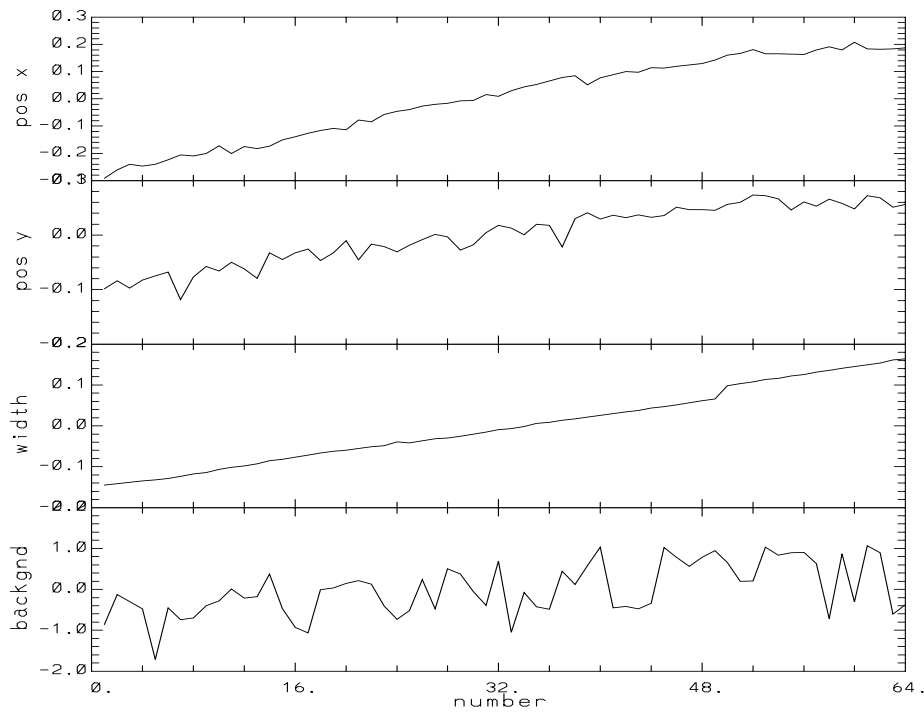


**Figure 2:** Time variation of the four external parameters characterizing the data. From top: *pos x* is the relative offset position in pixels of the spectra in the dispersion direction, *pos y* is the relative offset position in cross-dispersion, *width* is the mean relative change in the Gaussian sigma width of the spectrum, and the *background* shows the relative fluctuations of a data area mean in  $e^-$  per pixel.

The cross-dispersion position and width of the  $\alpha$  Cen B spectrum have been developed for each of the 64 spectra by fitting a Gaussian over 7 pixels in cross-dispersion at each dispersion column. Offset positions in the dispersion direction have been evaluated by determining what Fourier domain shift of a mean extracted spectrum (for A & B separately then averaged) is required to best match each of the individual 64 spectra. Figure 2 shows in time order the offsets along the dispersion (pos x), cross-dispersion (pos y), the Gaussian sigma for the  $\alpha$  Cen B order width (after subtracting the mean), and the background fluctuation level. The drift along the dispersion most likely results from Doppler motion over the *HST* orbit. The pixel scale is 25 km/s, and over an orbit Doppler motions of up to  $\pm 7.5$  km/s can result. (Note that observing in the CVZ would have prevented substantial Doppler offsets, since the telescope is pointed near the orbital pole.) At a spatial pixel scale of  $0''.05$  the  $< 0.2$  pixel drift in cross dispersion translates to  $0''.01$  which is typical for orbital offsets, and the small jitter on both the  $x$  and  $y$  positions is at a level expected from small *HST* guiding errors. Although a 0.5 pixel drift along the dispersion is a much larger change in a short period of time than desired for testing S/N in excess of 10000, it is expected from these non-CVZ observations. The strong variation of Gaussian width is apparently a result of *HST* OTA "breathing" which for the 36 minute interval of observations showed a negative focus change of 3.0 microns (M. Lallo, private comm.). The near-UV PSF is extremely sharp, and therefore sensitive to minor focus shifts.

To further demonstrate the variation of spectral order widths Figure 3 shows the Gaussian sigma values for all 64 spectra and each CCD column (after smoothing individual values for each spectrum over a 20 pixel scale along the columns). Time increases upwards in Figure 3. The apparent gap three quarters of the way through the sequence corresponds to a delay of three minutes in the observational cadence to allow the STIS data buffer to be dumped. At low column number the degradation of image sharpness from early in the sequence to late is easily seen from inspection of the 2-d images. The change at low column number results in the central pixel energy fraction (for spectrum centered on a pixel) dropping from 44% to 30%. The minor undulations result from a combination of effects including occasional saturation of the central pixel, the results of cross-dispersion offsets coupling with under sampled data, and the local spectrum intensity. The spectral order slopes across 7.5 pixels in cross-dispersion from left to right; the primary broadening of the Gaussian width cannot result from under-sampling coupled with a sub-pixel cross-dispersion drift.

Further investigation (existing Analyses pointed out by R. Kimble, private comm.) has shown that the G430M grating has an intrinsic, strong gradient in cross-dispersion FWHM versus wavelength for nearly all central wavelength settings (Bowers, et al. 1998). Such an intrinsic focus dependence with wavelength is not present in other STIS modes. The large and wavelength dependent drift observed for the cross-dispersion width is thus well explained as a combination of factors: (a) observing in the near UV where the intrinsically sharp point spread function is most sensitive to minor focus changes, (b) an intrinsic focus

gradient within the STIS G430M mode, and (c) chance observing during an interval of unusually strong monotonic changes of HST focus due to telescope “breathing”.

One unlikely possibility to explain the focus drift -- CCD heating from the high flux of  $\alpha$  Cen A UV photons -- was directly explored. Even if all the photons from 36 minutes were instantaneously deposited in only one row of the CCD, the temperature increase of that row would be only  $\sim 10^{-5}$  degrees K. Photon heating from the stellar source falls many orders of magnitude short of being a potential factor.

One reason that high S/N observations might be considered well matched to *HST* capabilities is the generally stable nature of observing conditions. The superb guiding with *HST* means that images can be repeated over long periods of time with offsets held to a fraction of a pixel. Thermal drifts are largest at the beginning of an observing sequence as *HST* and the science instruments equilibrate to a new thermal environment, therefore a one orbit test can be expected to provide worst case conditions. Unfortunately in this instance the drift in Gaussian width is unusually large, and does not provide conditions conducive to reaching the highest possible time-series differential S/N.

For longer observing sequences, even with the unusually susceptible G430M mode, the level of width changes induced by breathing should on average be smaller by a factor of two. In addition a longer sequence would better support identification and removal of any correlated noise in the photometry that might follow from this effect.

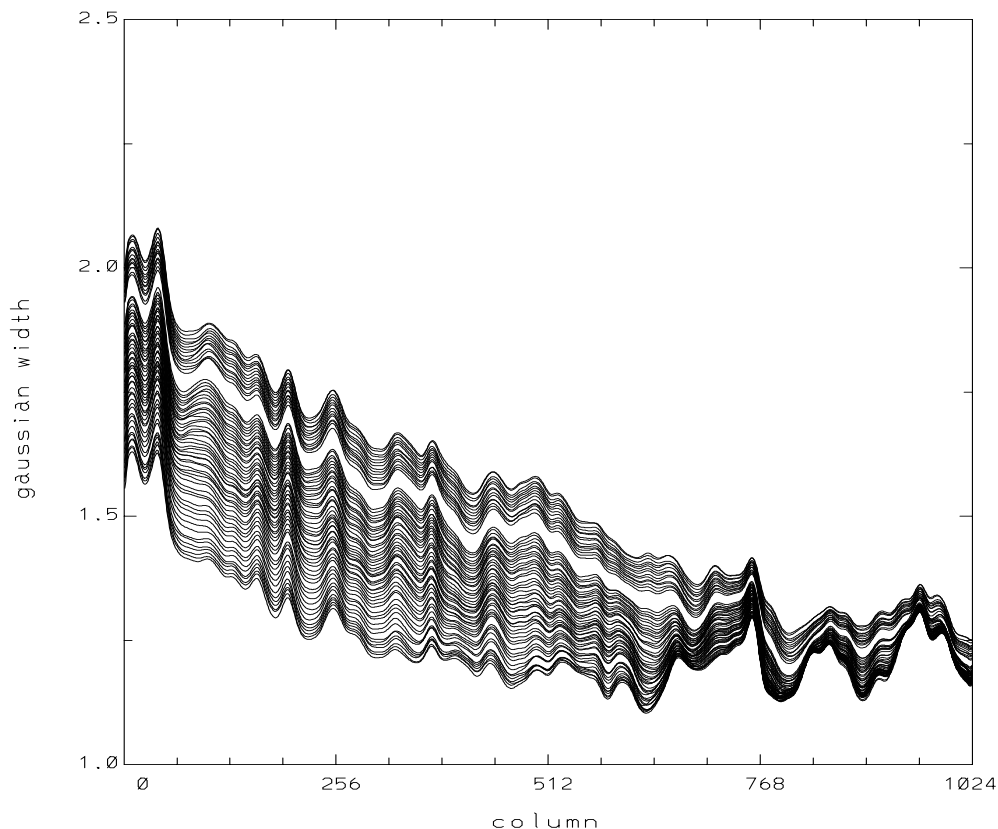


**Figure 3:** Further detail on the change of spectrum width as quantified by a Gaussian sigma width with CCD column on the ordinate. The width apparently increases linearly with time with a magnitude that is much larger at low column number than at high column number. Inspection of the 2-d images is consistent with interpreting this as a progressive focus change over the orbit.

Figure 4 shows the time record of counts for A & B after subtracting and normalizing to the global mean value of  $1.40 \times 10^9 e^-$  for  $\alpha$  Cen A and  $1.92 \times 10^8 e^-$  for  $\alpha$  Cen B respectively, and multiplying by 100 to express as percentage change. These extractions started at column 78 and ended at column 946 a range selected to start and stop well away from the CCD boundary (the CCD well depth drops off around the periphery) and at locations where both the A & B spectra are flat (therefore sum is not sensitive to minor dispersion offsets). An 11 pixel box centered on the spectrum in cross-dispersion was used to extract  $\alpha$  Cen B and a 31 pixel box was used for  $\alpha$  Cen A. The data have been flat-fielded, although this step made little difference in the results. (The flat fields were applied to the extracted spectra by dividing by the flat field averaged over cross dispersion with the intrinsic order line spread function. Thus for  $\alpha$  Cen A the flat field matches the input pho-

ton distribution, not the resulting photoelectron distribution dominated by bleeding along columns.)

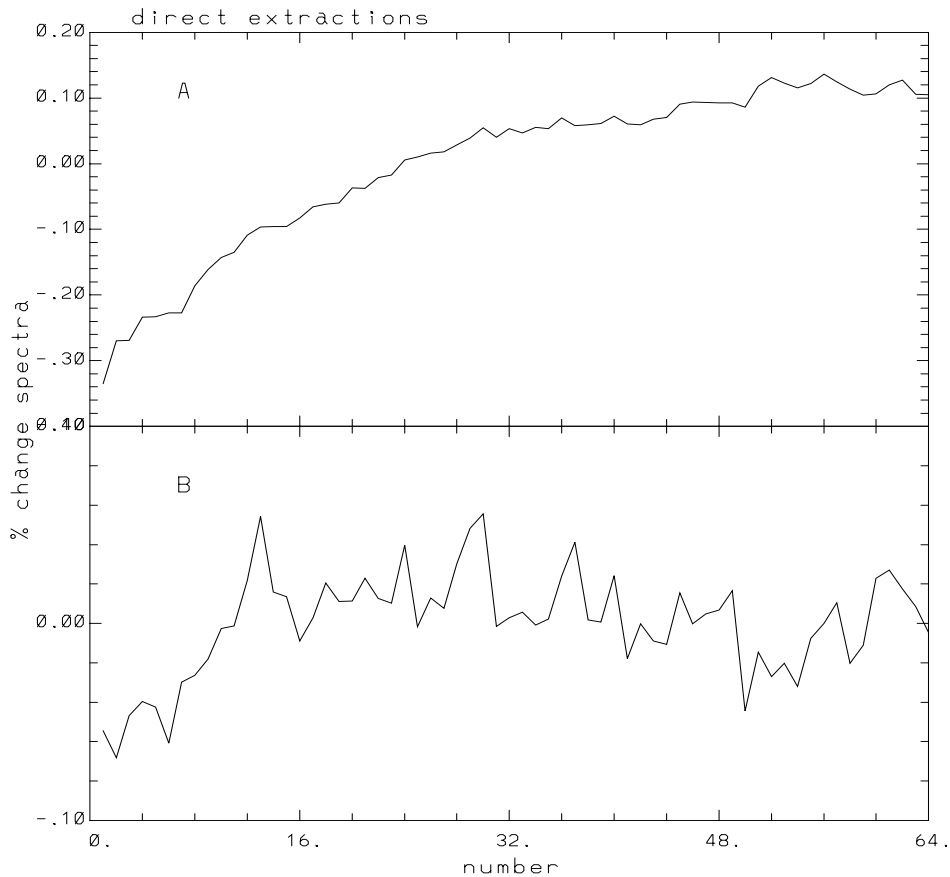


**Figure 4:** Time series variation for extracted  $\alpha$  Cen A and  $\alpha$  Cen B spectra as %. An *rms* deviation in this figure of 0.01% would correspond to a S/N of 10000.

The character of change for the  $\alpha$  Cen A & B spectra are different from each other, and each in turn is different from variation of the external parameters shown in Figure 2. Although extraction boxes have been selected to minimize sensitivity to minor changes of position, or width it would not be surprising for variations in these parameters to introduce correlated noise. It is common procedure in time series analyses to remove any fluctuations in stellar time series that correlate with obvious external parameters. In this case it is clear from inspection of Figures 2 and 4 that some of the large scale change in A and B does not correlate with these external parameters. For example the first  $\sim 11$  exposures of B show a strong upward trend while no corresponding feature appears in the external parameter traces. The time series for A shows significant curvature, suggestive of a relaxation process to an asymptote, while no corresponding feature appears in the external parameters. If the change in A followed from a drift in the CCD gain, or the exposure times, then it should appear in B as well.



Despite larger instrumental drifts than anticipated, it is still instructive to consider what S/N levels result from various analysis prescriptions. At the simplest level S/N for A and B follows from the direct ratio of mean count level to the associated *rms* for the full time series as shown in Fig. 4 -- this results in S/N of 843 and 3826 for A and B respectively. Such an analysis almost surely underestimates the real S/N (where "real" should be thought of as scientifically useful) that has been obtained and would likely result from extended, similar observations.

In the next section a time series analysis will be pursued that involves removal of obvious data trends and removal of any noise correlated with the well measured external parameter time series.

#### 4. Time Series Results

Before launching into operations on the time series of photometry it will be instructive to consider possible sources of noise. One irreducible noise source exists -- the random fluctuations from Poisson noise that will equal square root of the number of detected photons. With  $1.4 \times 10^9 e^-$  per  $\alpha$  Cen A spectrum and  $1.9 \times 10^8 e^-$  per  $\alpha$  Cen B spectrum the Poisson noise will result in relative *rms* fluctuations of  $2.7 \times 10^{-5}$  and  $7.3 \times 10^{-5}$  respectively. Variations of x,y position and spectral order width will generate intensity changes in two general ways. The discussion to follow develops the expected correlated noise from these external parameter changes to better than order of magnitude accuracy, but probably not better than a factor of two:

The two ways in which intensity fluctuations are generated are:

1. The change leads to a direct change in flux contained within an extraction box fixed in pixel space.

For changes in dispersion position this sensitivity has been forced to nearly zero by selecting end points in dispersion at flat parts of the spectra of both A & B. Direct changes from a 0.5 pixel offset (in the direction seen) in x should be  $4 \times 10^{-5}$  (A) and  $1 \times 10^{-4}$  (B). These peak values which are near the Poisson limits to start with would follow from the near linear drift over the 36 minute observing interval. From Figure 2 it is clear that high frequency fluctuations about this trend are several times smaller; these should produce fluctuations in intensity several times smaller than Poisson noise and therefore should not be an important determinant of final S/N.

For changes in cross-dispersion position the extraction boxes of 31 and 11 pixels for A & B are large enough to both include most of the flux and to extend to a region of generally symmetric and gently sloping wings. Direct estimates of sensitivity to the full range of position in y = 0.15 pixel offsets are  $1 \times 10^{-5}$  and  $2 \times 10^{-4}$  (B). The flux in A is concentrated to the saturated pixels and the wings are symmetric; there should be no detectable induced response for A. The wings for B are slightly skewed by the back-

ground from A being larger on the positive rows, the full range drift should induce an increase of  $\sim 2$  parts 10000, the smaller superposed fluctuations in the y-position should be near or below the Poisson noise level for B.

The effect of a changing width is more difficult to reliably estimate. However, for A the extraction box height is large (forced by need to comfortably include longest bleeding columns) compared to the intrinsic order width. Also inspection of wing heights near the extraction box edges show no sensible change from the beginning to end of observing. No detectable response is expected for A. For B the wing intensity (averaged above and below) shows a slight increase of  $\sim 18 e^-$  per pixel from the first to last exposure, assuming this should apply to a range of  $\sim 15$  pixels cross dispersion would imply a full range drop of extracted intensity of  $\sim 1.2 \times 10^{-3}$  (perhaps with factor of two confidence in magnitude). The increased flux in the wings presumably balances a drop in flux within the extraction box. There should be a noticeable change in the apparent intensity of  $\alpha$  Cen B as a result of the broader cross-dispersion profiles with time. Since (see Figure 2) the relative noise level of the width compared to the drift is very small, any high-frequency noise added to the B time series should be small.

2. Changes of position or width lead to intensity changes as a result of imperfect correction for flat-field or other CCD pixel-to-pixel response corrections interacting with motion of sharp pixel-to-pixel intrinsic flux differences and motion.

The STIS/CCD has a very flat response. Even in the UV (an estimated flat-field for  $3305 \text{ \AA}$  was created by averaging together two pre-launch, archival flats [i4g1725kopfl and i4g1725lopfl] at  $3165 \text{ \AA}$  and  $3423 \text{ \AA}$  respectively) the typical pixel-to-pixel flat-field *rms* is  $\sim 0.008$ . The stellar intensity falls on  $\sim 3$  pixels cross dispersion, with the 869 pixel extraction box this implies  $\sim 2600$  pixels are averaged over. Since pixel-to-pixel intrinsic intensity differences are order unity for these under-sampled spectra the response to flat-field induced signal if flat-fielding is not applied, or the flat-field noise is comparable to typical deviations should be  $\sim 0.008/2600^{1/2} \sim 1.5 \times 10^{-4}$  per 1 pixel shift. Since the cross dispersion drift is only 0.15 pixel the effect here should be  $\sim 2.4 \times 10^{-5}$ . In the dispersion direction the 0.5 pixel drift coupled with pixel-to-pixel changes that are in reality only 0.25 the mean intensity, would translate to a full range relative amplitude change of  $\sim 2 \times 10^{-5}$ . Indeed little difference is seen analyzing the time series with or without flat-fielding. (Close inspection of the flat field does not show any significant features near the spectral order centers.) Fluctuations point-to-point in the time series should be smaller yet and well beyond the Poisson limit.

To sum up regarding expected correlated noise on the  $\alpha$  Cen A and  $\alpha$  Cen B spectra associated with the well measured x,y positions and order width as plotted in Figure 2: The only significant trend should be a roughly linear decline of order 0.1% in  $\alpha$  Cen B as a result of the increasing order width. Other trends and induced fluctuations should usually be only near and often below the small Poisson noise limit. With a substantial number of

points in the time series searching for such correlated noise, and removing it if it is present, is a valid and worthwhile exercise.

The unique shapes of the  $\alpha$  Cen A and  $\alpha$  Cen B time series in Figure 4 with respect to the shapes of the external parameter changes in Figure 2 require consideration before any meaningful attempt can be made to estimate and remove noise induced by the x,y and width variations. Noting that the shape of the  $\alpha$  Cen A time series in particular has the appearance of an exponential relation, I have tried fitting each of the Figure 4 series with an exponential -- Figure 5 shows the results.  $\alpha$  Cen A is fit by:

$$Int_i = 0.1271 - 0.4630 \times \exp(-t_i/18.88)$$

where  $Int_i$  are the % changes as in Figure 4, and the  $t_i$  are a time-like sequence simply set to the exposure number (except with a gap of 5.8 introduced where a real 3 minute gap corresponds to 5.8 steps which average 30.8 seconds). The time series of  $\alpha$  Cen A is remarkably well fit by a simple exponential relaxation with a (physical) e-folding time of 9.7 minutes. The fit is so good that the resulting S/N, measured simply as the ratio of mean to residual *rms* jumped from 843 to 8498! Although lacking a known physical explanation for the behavior of the  $\alpha$  Cen A time series, it is a safe conclusion that it represents some aspect of the CCD micro-physics perhaps associated in a unique way with observing in a rapid time series with over-saturation. In any case subtracting the exponential fit before proceeding with regressions against x,y positions, width, and background is a reasonable step.

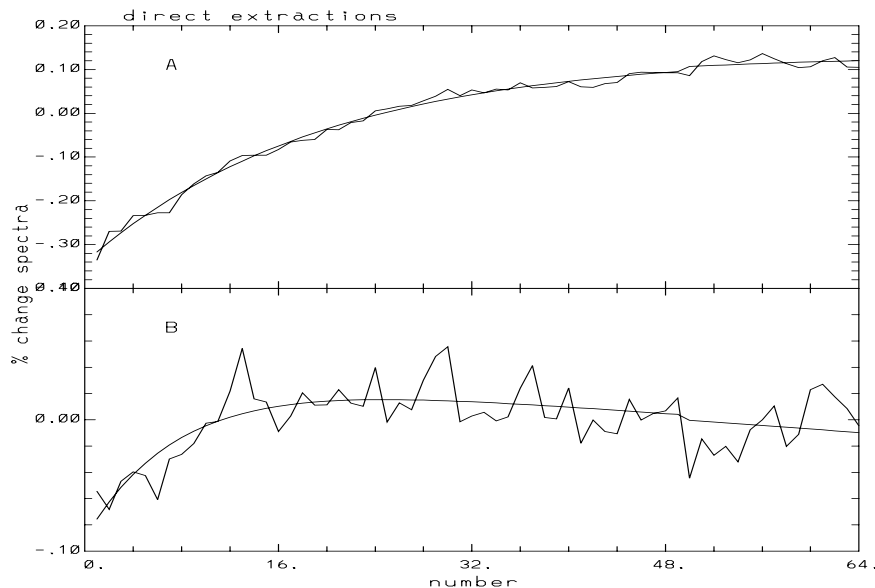


**Figure 5:** Same as Figure 4 with superposition of best fitting exponential (and linear term for  $\alpha$  Cen B) functions as discussed in the text.

For  $\alpha$  Cen B a linear term has been included since such is expected from the change of spectral order width with time, the resulting fit is:

$$Int_i = 0.0157 - 0.1275 \times \exp(-t/7.76) - 6.74 \times 10^{-4} \times (t_i - 32)$$

For  $\alpha$  Cen B inclusion of the exponential + linear fit improves the S/N from 3825 to 5332, a more modest, but still significant gain. In this case the “model” of an exponential relaxation process is less obvious, although the fit to the data is clearly decent. (A speculation: perhaps the same process in both cases leads to a minor exponentially decaying non-linearity, and it has a larger amplitude and time scale with involvement of a larger number of pixels at high photo-electron levels. CCD surface micro-physics of change traps being filled in?) For general considerations it would be of interest to know the time scale on which the exponential nonlinearity resets. The only evidence here is that over a 3 minute gap in the observing series the trend continues at full amplitude. The time scale to reset must be long compared to 3 minutes.

A S/N is generally evaluated here as the mean of a time series quantity divided by the root mean square *rms* variation of that quantity about the mean. The *rms* is evaluated as  $\sqrt{\text{sum of squares}/\text{number of independent measures}}$ , where the number of independent measures is taken as the number of points in the time series minus the number of parameters fit out before evaluating. For example if an exponential fit is used to flatten a vector, and then it is linearly regressed against three external parameter vectors the number of independent measures is reduced by six. (For example the quoted  $\alpha$  Cen A S/N of 8498 is already reduced in this way, based on direct time series mean and *rms* the S/N would be 8704.)

In general S/N will be quoted at four different stages:

1. Direct extraction as plotted in Figure 4.
2. After removal of an exponential function fit (Figure 6).
3. After decorrelation against a combination of the vectors shown in Figure 2. (Used x,y and background only, the correlations with the width were always insignificant. The x,y and background vectors were detrended with a linear fit before correlating with the already detrended stellar vectors.)
4. After any correlation between the resulting A and B vectors are removed from each other as shown in Figure 7. (This can correct for correlated noise that might follow from any other sources such as drifts in gain that would affect both stars equally.)

Table 1 provides S/N from top to bottom for the four cases just enumerated for  $\alpha$  Cen A & B.

**Table 1: Time Series Signal-to-Noise Result.**

<b>Case</b>	<b>A</b>	<b>B</b>	<b>Comment</b>
1	843	3825	Direct series.
2	8498	5332	Exponential subtracted.
3	8839	6422	x,y, background regressions.
4	9444	6860	A by B, and B by A regressions.

Correlation coefficients of the  $\alpha$  Cen A and  $\alpha$  Cen B time series with the external parameters are shown in Table 2.

**Table 2: Linear Correlation Coefficients.**

<b>Star</b>	$r_{x-pos}$	$r_{y-pos}$	$r_{backgnd}$	$r_{A,B}$
A	0.082	0.177	0.322	0.373
B	-0.261	-0.522	0.180	0.373

All of the correlations (except  $r_{x-pos}$  for A) are statistically significant. The 0.373 linear correlation of the A and B series after removal of the other terms suggests that either: (1) significant noise on some of the x,y and background vectors left uncorrected and still correlated noise in both stellar vectors, or (2) other relevant external forcing functions common to both stars exist.

Cases were also analyzed with extraction boxes limited to a smaller y-domain, e.g. columns 504 to 946, and also sets with slightly different vertical extents. In general the resulting S/N values were similar, but lower by a few percent than those in Table 1.

The Poisson limit S/N for the cases in Table 1 are 37400 and 13850 for A and B spectra respectively. The results are still a considerable distance from the limiting S/N.

It is probable that results from more extensive observations after the instrument has thermally stabilized would allow higher S/N to be obtained. S/N inferred from the central 32 pixels in Figure 7 corresponding to a smaller range of external parameter variation are 10932 and 8805 for  $\alpha$  Cen A and  $\alpha$  Cen B respectively.

## 5. Summary

CAL/STIS-8438 provided data to further probe the capability of reaching ultra high S/N with the STIS/CCD in a time series mode. The large range of drift in the projected position of spectra on the CCD, and especially of an apparent spatially dependent focus change with time have compromised obtaining robust results. Nonetheless results close to S/N =

10000 per exposure have been obtained; this corresponds to the level at which the capability becomes very interesting for asteroseismology.

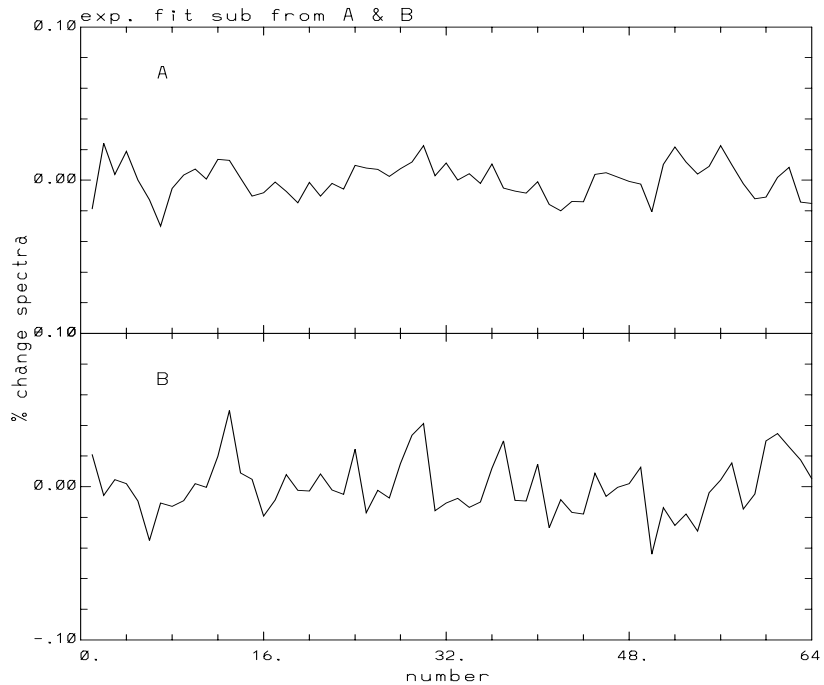


**Figure 6:** Residuals after subtracting the exponential fits as shown in 5.

It seems likely that:

1. Saturated spectra can support S/N at least as high as unsaturated data (with possible need to allow for a unique transient associated with saturated data).
2. For exposure times of 10 seconds and near S/N of 10000 there is evidence of a moderate correlation in the A and B spectra from unexplained sources that could compromise attempts to obtain ultra high S/N results on single sources. (However, the presence of one star can induce noise in the other as well, so this is a problematic conclusion.)
3. With sufficient counts to support this, and stable observations (use of CVZ to minimize dispersion position drifts, and observing at the same position for several orbits to allow initial thermal fluctuations to damp out) S/N in excess of 10000 can be obtained.

Only with substantially more extensive observations, such as the 15 orbits in GO-8115 (PI Valenti) attempting to obtain science results on a star with expected oscillation ampli-

tudes well above solar, can some of the uncertainties arising from this one orbit test be addressed.

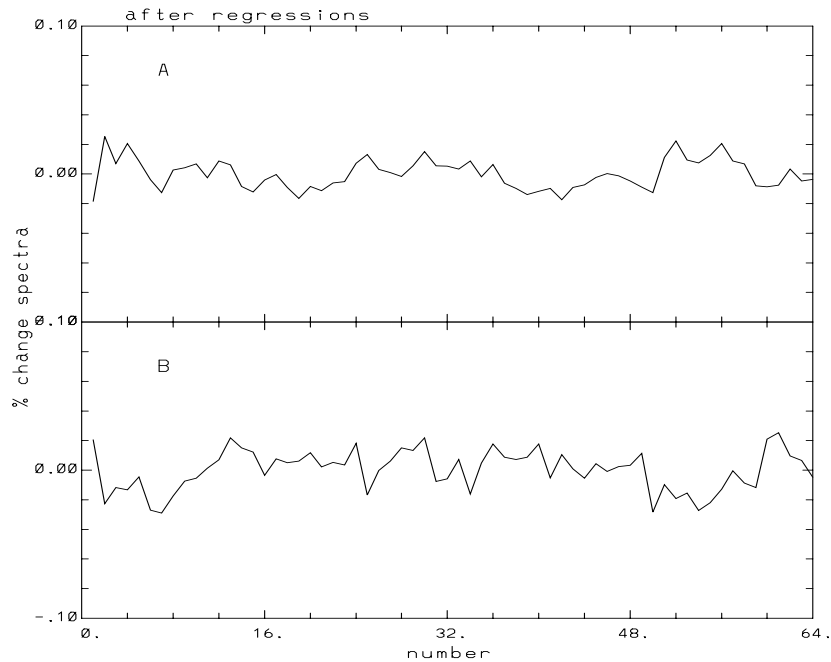


**Figure 7:** Residuals from Figure 6 further reduced by removing any noise that was correlated with  $x,y$  position and background intensity variations and with the resulting  $\alpha$  Cen A and  $\alpha$  Cen B time series regressed against each other. These time series correspond to the S/N entries for the last line in Table 1, a S/N of 9444 for A and 6860 for B.

## 6. References

- Bowers, C. et al. 1998, SPIE 3356, p. 401
- Gilliland, R.L. et al. 1993, AJ, 106, 2441
- Gilliland, R.L., Goudfrooij, P. & Kimble, R.A. 1999, PASP, in press